PHYSICAL REVIEW B VOLUME 43, NUMBER 2 15 JANUARY 1991-I

Femtosecond excitonic bleaching recovery in the optical Stark effect of $GaAs/Al_xGa_{1-x}As$ multiple quantum wells and directional couplers

S. G. Lee,* P. A. Harten, J. P. Sokoloff, R. Jin, B. Fluegel, K. E. Meissner, C. L. Chuang, R. Binder, S. W. Koch,* G. Khitrova, H. M. Gibbs, and N. Peyghambarian
Optical Sciences Center, University of Arizona, Tucson, Arizona 85721

J. N. Polky
High Technology Center, Boeing Electronics Co., Seattle, Washington 98124-6269

G. A. Pubanz
Oregon State University, Corvallis, Oregon 97331
(Received 23 July 1990)

Femtosecond pump-probe spectroscopy was used to study the ultrafast-excitonic-bleaching-recovery feature in the optical Stark effect of several $GaAs/Al_xGa_{1-x}As$ multiple-quantum-well samples at room and low temperatures. We also have seen this effect in a nonlinear directional coupler as a total transmission increase of the waveguides. The semiconductor Bloch equations for the system were solved numerically and gave good qualitative agreement with the experiments. The transient absorption saturation and recovery observed in the experiments is explained as an ultrafast adiabatic following of the semiconductor excitation.

INTRODUCTION

One of the simplest and most powerful ways of studying a semiconductor optically is the pump-and-probe technique. When using this technique the temporal resolution of the experiment, i.e., the laser pulse width, determines to what extent carrier dynamics, as well as optical coherent transients, must be considered when interpreting the data. For instance, nanosecond and longer-pulse laser sources provide information on the steady-state properties of excited electronic systems. Under steady-state conditions the pump pulse is just a convenient way to prepare the system; carriers generated in this way have no memory of how they were generated. This is not always the case with femtosecond (fs) pulses, however, for if the pulse duration is less than or on the order of the relaxation times within the semiconductor, then probe pulses actually yield information on the coherent light-matter interactions within the semiconductor.

Previous studies of coherent transition experiments in semiconductors include photon echoes using 6 fs pulses[1] and the optical Stark effect.[2–7] In these excitonic Stark effect experiments a fast reduction, or bleaching, of the exciton absorption line is always observed to accompany the Stark shift. Although this bleaching does not completely recover on a fs time scale, it has a component which lasts no longer than the duration of the pump pulse. In this paper we study this fast bleaching recovery in the optical Stark effect of GaAs quantum wells and nonlinear directional couplers more closely, and show that it can be interpreted as transient adiabatic following.

Adiabatic following[8–10] is an off-resonant effect which occurs when the duration of a light pulse is less than the phase relaxation time, T_2, and the magnitude of the pulse detuning is greater than its inhomogeneous linewidth. Under these conditions the quantities in the optical Bloch equations which describe the system, namely the inversion and polarization, have a time dependence determined by the instantaneous amplitude of the light pulse envelope, i.e., they follow the field.

The above conditions on the pulse duration and detuning can be satisfied in a semiconductor using fs laser systems. This is most easily achieved for the exciton resonance in GaAs multiple-quantum-well structures (MQW's), which have a coherence time approaching one picosecond. The response of the exciton to a nonresonant light pulse can be described by the inversion, and interband polarization, of the system using the semiconductor Bloch equations,[11–16] which include the many-body Coulomb effects in time-dependent Hartree-Fock approximation. The numerical solution of these coupled equations not only explains the Stark shift, as shown previously,[11–16] but also indicates that the system's inversion adiabatically follows the field.[10] This aspect of the Stark effect is manifested experimentally in the time-resolved absorption measurements as a fast bleaching recovery of the exciton line and as a transmission increase at zero time delay in a GaAs quantum-well nonlinear directional coupler (NLDC), as will be shown here.

EXPERIMENT

Time-resolved pump-probe experiments were carried out using a synchronously pumped mode-locked dye laser with an average output power of 25 mW, 82 MHz repetition rate, and center wavelength tunable from 850 to 870 nm for room-temperature experiments. A colliding pulse mode-locked (CPM) dye laser amplified by copper vapor lasers (CVL) in cascade operating in 750–800 nm was employed for low-temperature ($\cong 10$ K) experiments. The arrangement for the room-temperature experiments on MQW's and NLDC used an acousto-optic modulator (AOM), which had a 1-μs duration and 0.01 duty cycle. The AOM was placed in the beam immediately after the laser cavity to prevent thermal buildup in the sample by the high repetition laser. Based on an assumed sech^2 shape, autocorrelation measurements indicate that the AOM temporally broadens the initial 60-fs pulses to 260 fs. The pump-and-probe pulses were collinear and had orthogonal polarizations. For low-temperature experiments, we first generated a continuum using CPM pulses amplified by CVL and then the near-IR pulses were obtained by reamplifying the desired portion of the generated continuum using a second CVL. The autocorrelation of the pump pulse and the cross correlation of the pump-and-probe pulses in this case were 200 and 300 fs, respectively. The samples were molecular-beam epitaxy (MBE) grown $GaAs/Al_xGa_{1-x}As$ multiple-quantum-well and multiple-coupled-quantum-well structures (MQW's and MCQW's) with various well widths and barriers. In all room-temperature measurements the laser center wavelength was adjusted so as to be detuned by between four and five E_R below the heavy-hole exciton. Here E_R is the bulk GaAs Rydberg energy, i.e., 4.2 meV. The detunings for low-temperature measurements were smaller. The spectral transmission of the probe through the sample, for different time delays between pump and probe, was measured by an optical multichannel analyzer at the output of a spectrometer.

GaAs MQW

Figure 1 shows the low-temperature absorption spectrum of a GaAs MCQW sample for pumping below the exciton resonance and for different time delays, t_p, where $t_p = t(\text{probe}) - t(\text{pump})$. The solid curve represents the linear absorption, while the dotted spectrum corresponds to $t_p = 0$. It clearly shows the heavy-hole exciton has been blue shifted and bleached. The $t_p = 0$ coincides with the time delay of maximum exciton bleaching, *not* maximum exciton Stark shift. The latter is consistently seen at negative delay times, both in experiments and theoretical calculations.[5] In general, it occurs when the probe comes just before the pump pulse, so that the probe polarization can be affected by the entire subsequent pump pulse, and it has not yet undergone significant dephasing when the pump pulse arrives. The dashed curve in Fig. 1, which corresponds to $t_p = 500$ fs, demonstrates that the blue shift and bleaching are mostly recovered. The complete recovery takes nanoseconds as a result of carrier generation caused mainly by the spectral overlap of the pump and the sample's absorption spectrum. The transient exciton blue shift is a consequence of optical Stark effect and has been discussed in earlier publications.[2–7] The ultrafast exciton bleaching and recovery that accompanies the blue shift have also been seen[2–7] but have not been explained. This bleaching recovery cannot be a result of the exciton versus free-electron–hole pair phase-space filling effect.[17,18] In that case, the dominant bleaching recovery occurs due to exciton ionization into electron-hole pairs. Since the exciton ionization time is much longer than a few hundred femtoseconds at low temperatures, and furthermore, since our bleaching recovery signal, following the dynamics of the pump pulse, has a less than 500-fs duration, we can safely rule out these exciton phase-space filling effects as an interpretation of our data. We attribute the origin or the fast bleaching recovery to transient adiabatic following as ex-

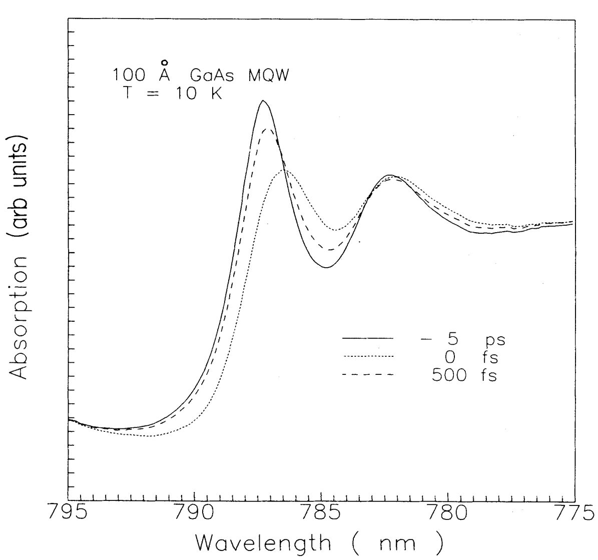

FIG. 1. The absorption spectra of a MCQW at $T = 10$ K at different time delays. The pump wavelength was centered at 793 nm. The sample had the repeated unit 198-Å $Al_{0.13}Ga_{0.87}As$/47-Å GaAs/3-Å AlAs/47-Å GaAs. (The asymmetric states lie outside the spectral range shown.)

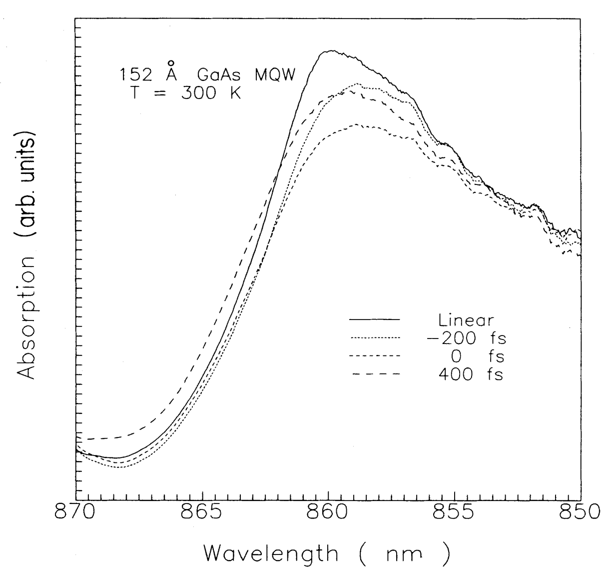

FIG. 2. Room-temperature transient absorption spectra of 152-Å GaAs MQW. The heavy-hole exciton linewidth was difficult to determine due to the closeness to the light-hole exciton. The detuning was $4.7E_R$.

plained in the discussion section of this paper.

The exciton dynamics for off-resonant excitation at room temperature is very similar to the low-temperature observations. Figure 2 shows our room-temperature results in a 152-Å GaAs MQW for a pump-exciton detuning of $\cong 4.7E_R$. While the Stark shift, which reaches its maximum magnitude at $t_p = -200$ fs, recovers completely at $t_p = 400$ fs, the excitonic bleaching only partially recovers. The fast component of bleaching recovery again follows the pump-pulse dynamics.

Nonlinear directional coupler

The ultrafast bleaching recovery in the optical Stark effect has also been observed in a GaAs/$Al_xGa_{1-x}As$ NLDC at room temperature. The structure of the NLDC and its operation have been explained in Ref. 19 in more detail. The coupler consists of two waveguide channels with 2 μm spacing and length of 1.24 mm. The 1.2-μm-thick guiding region of the NLDC consists of 60 periods of 100-Å GaAs/100-Å $Al_xGa_{1-x}As$ MQW layers. The guiding in the vertical direction is achieved by two $Al_xGa_{1-x}As$ layers with lower effective indices above and beneath the MQW region. Reactive ion etching of pairs of ridge guides on the top of $Al_xGa_{1-x}As$ layer results in channel definition of the NLDC. The data were taken by imaging the NLDC output end on the charge-coupled device (CCD) array of the optical multichannel analyzer directly. The inset of Fig. 3 schematically shows the geometry for operation of the NLDC. The probe pulses, which are coupled to channel 2 of the NLDC, cross couple into channel 1 for a certain length of the channel, called the critical length. However, the application of a pump pulse in channel 2 results in destruction of this coupling as the index of refraction in the guiding region is changed, forcing the probe light to stay in channel 2. A typical NLDC behavior is shown in Fig. 3, where the normalized transmission of the two channels is plotted as a function of the input intensity of the pump pulse at a fixed time delay. As expected at low pump intensities, the probe light that was originally coupled into channel 2 is cross coupled and exits from channel 1. Due to the use of pulsed excitation,[20,21] and since the length of the waveguide is probably not completely optimized, not all the probe light is coupled to channel 1. As the pump intensity is increased, we clearly see the coupling back from channel 1 to channel 2. The dynamics of this nonlinear directional coupling operation may be measured in a time-resolved pump-probe experiment. Figure 4 displays such an operation, where the output intensity profiles are plotted for different time delays between the pump and the probe pulses. At large negative time delays, for which the probe leads the pump, most of the probe exits the device through channel 1 after cross coupling. At zero time delay it is switched back to channel 2 as a result of pump action. For large positive delays it returns to its initial path. Figures 3 and 4 show that we are able to obtain a *transient* (i.e., < 1-ps recovery) crossover in the output intensity ratio of the two channels at a pump intensity of about 2 GW/cm^2.

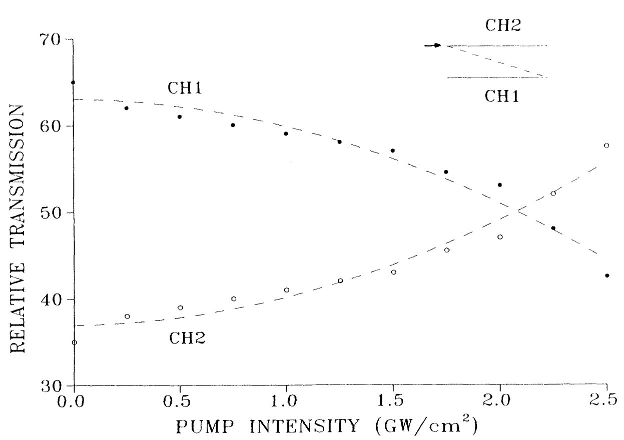

FIG. 3. Relative probe transmission of the two channels as a function of pump intensity at a fixed time delay. The intensities are normalized by the transmitted total intensity. The inset shows the probe beam propagation direction without a pump beam.

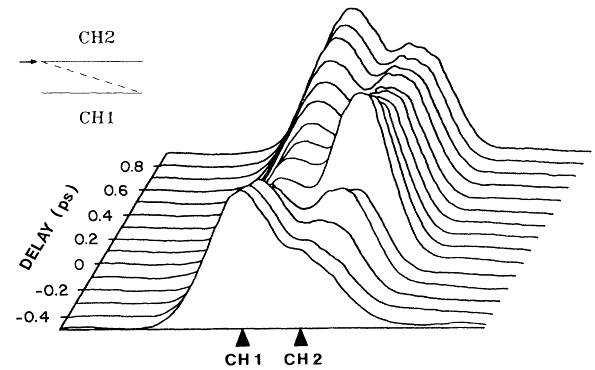

FIG. 4. NLDC output intensity profiles for different time delays. The pump intensity was about 2 GW/cm^2.

In the NLDC experiment, the ultrafast change in the absorption coefficient (α) of the sample usually manifests itself as a change in its transmission (T), which can be expressed as $T = \eta(1-R)^2\exp(-\alpha L)$, where η is the mode coupling and guiding efficiency, R is the reflectivity of the input and output faces, and L is the length of the sample. Because of the relatively long coupling length ($L \cong 1-2$ mm) necessary for the operation of the NLDC, a direct observation of the nonlinear processes near the exciton peak, where $\alpha L \gg 1$, is not possible. However, the large L makes the device very sensitive to relatively small changes of α since $\Delta T/T = -\Delta\alpha L$. For example, $\Delta\alpha = -3$ cm^{-1} is needed for $\Delta T/T = 0.3$. Such a small change in α is difficult to detect in a regular 1–2-μm sample, while it can be easily measured in our experiment, although for large detunings of 30–40 meV from the exciton peak.

The transient blue shift and bleaching of the exciton resonance in the optical Stark effect is expected to cause a transient *increase* in the total transmission of the NLDC ($\Delta T > 0$) if one assumes that the change of guiding

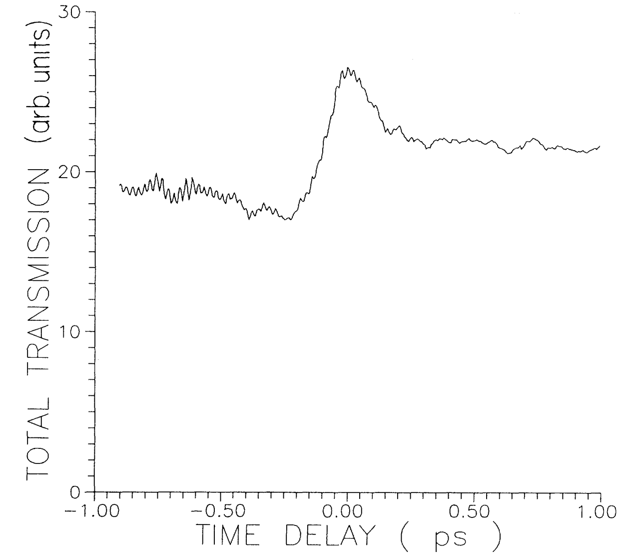

FIG. 5. Total transmission of NLDC as a function of time delay.

efficiency (η) is negligible. We indeed observed such a transient increase in the total transmission of the NLDC, as shown in Fig. 5, where a maximum $\Delta T/T>0.5$ is seen at zero time delay between the pump and the probe. The intensity and recovery time of this observation is in qualitative agreement with the result of our theoretical simulations, as discussed below.

The incomplete part of the signal recovery in Fig. 5 may be attributed to the generation of real carriers, either by one-photon or two-photon absorption. To distinguish between the two processes, we analyzed the dependence of the unrecovered part of the signal on the pump intensity. This incomplete-recovery component, which is roughly proportional to the carrier density, would vary quadratically with intensity for two-photon absorption and linearly with intensity for one-photon absorption in the exciton tail. The result is shown in Fig. 6 where the unrecovered part of the signal, i.e., the difference between transmission at $t_p=1$ ps and $t_p=-1$ ps, is plotted as a function of pump intensity. The inset of Fig. 6 displays the complete dynamics of the NLDC operation. The arrows in the inset represent the signal that is plotted in Fig. 6. It indicates that the two-photon absorption is negligible in our case, since the quadratic coefficient is much smaller than the linear coefficient in fitting the data. Thus, we conclude that generation of carriers by one-photon absorption is responsible for the incomplete recovery of our data.

DISCUSSION

For the analysis of our experiments, we use the semiconductor Bloch equations. These are the equations of motion for the expectation value of the population of the state, k, and interband polarization, $P_{\mathbf{k}}$. The Bloch equations describing the fs response are

$$i\hbar\frac{\partial}{\partial t}P_{\mathbf{k}}=\left[-\frac{i\hbar}{T_2}+\varepsilon_{\mathbf{k}}-2\sum_{\mathbf{k}'\neq\mathbf{k}}V_{\mathbf{k}-\mathbf{k}'}f_{\mathbf{k}'}\right]P_{\mathbf{k}}-(1-2f_{\mathbf{k}})\left[\sum_{\mathbf{k}'\neq\mathbf{k}}V_{\mathbf{k}-\mathbf{k}'}P_{\mathbf{k}'}+\mu E\right], \qquad (1)$$

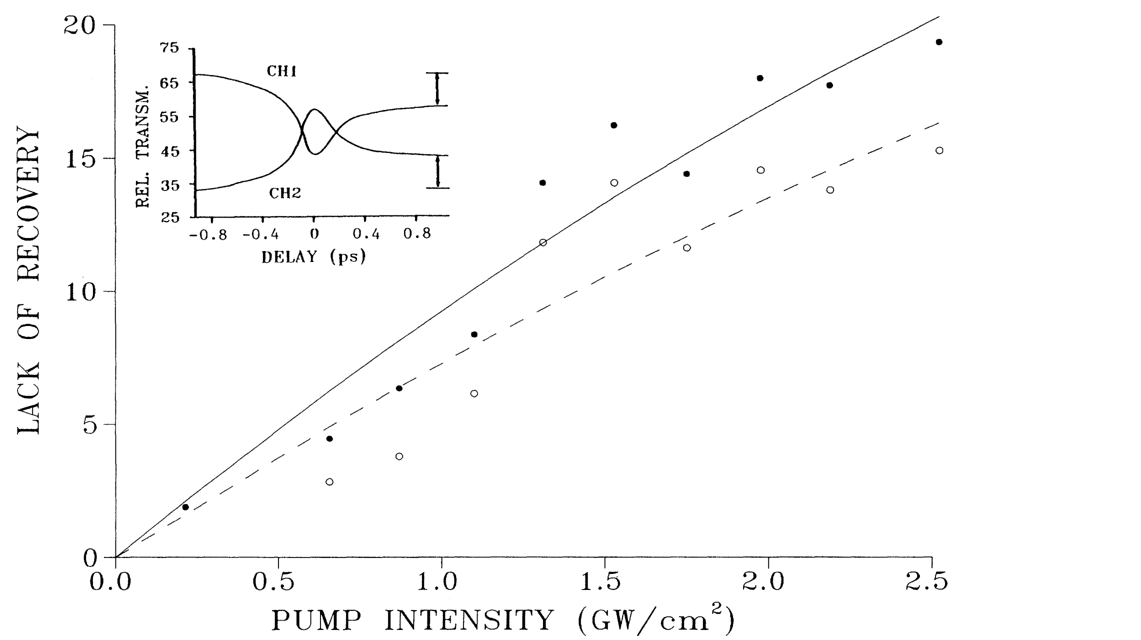

FIG. 6. The magnitude of the unrecovered signal as a function of pump intensity. The vertical axis is the difference between transmissions at $t_p=-1$ ps and $+1$ ps as shown in the inset by arrows. Open circles are for channel 1 (CH1) and solid circles are for channel 2 (CH2).

$$\hbar \frac{\partial}{\partial t} f_{\mathbf{k}} = -\frac{\hbar(f_{\mathbf{k}} - f_{\mathbf{k}}^0)}{T_1} + 2\,\mathrm{Im}\left[\left[\mu^* E^* + \sum_{\mathbf{k}' \neq \mathbf{k}} V_{\mathbf{k}-\mathbf{k}'} P_{\mathbf{k}'}^* \right] P_{\mathbf{k}} \right], \quad (2)$$

where $\varepsilon_{\mathbf{k}} = E_g + \hbar^2 k^2/2m - h\omega_L$, and ω_L is the central frequency of the excitation pulse. Here T_2 is the phenomenological phase relaxation time, T_1 is the longitudinal relaxation time, μ is the dipole interband matrix element, E is the electric-field amplitude in the rotating frame, and V is the Coulomb potential. Notice that when terms containing the Coulomb potential are ignored, the equations reduce to the optical Bloch equations for a set of inhomogeneously broadened two-level system, where the inhomogeneity is in k space, rather than real space. The additional Coulomb terms in (1) and (2) renormalize the system energy as well as the applied electric field inside the semiconductor.

We solved Eqs. (1) and (2) numerically for different time delays, ignoring the T_1 relaxation term because the pulse duration is much shorter than the carrier lifetime. The calculated spectrum for comparison with the room-temperature data of Fig. 1 is shown in Fig. 7. The material parameters are those of a 50-Å GaAs MQW with a $1.2E_R$ Lorentzian-shaped linewidth, irradiated by a 70-fs Gaussian-shaped pump, energetically detuned $7.3E_R$ below the heavy-hole exciton. As in the experiment, the pump-pulse duration and detuning satisfied the adiabatic following conditions mentioned earlier. The temporal behavior of the exciton in Fig. 7 shows good qualitative agreement with the data. That is, the exciton both bleaches and shifts at negative time delays. The Stark shift which reaches a maximum at a negative time fully recovers after several hundred fs, while the bleaching, which is maximized at $t_p = 0$, does not quite completely recover. Similar solutions of the Bloch equations, for comparison with low-temperature data of Fig. 2, are plotted in Fig. 8. Again good qualitative agreement between the experiment and theory is obtained.

In the calculations, the amount of the long-lived bleaching is determined by the dephasing rate in the vicinity of the pump-pulse frequency. Since a microscopic calculation of the frequency dependence of the homogeneous exciton broadening within the solution of the

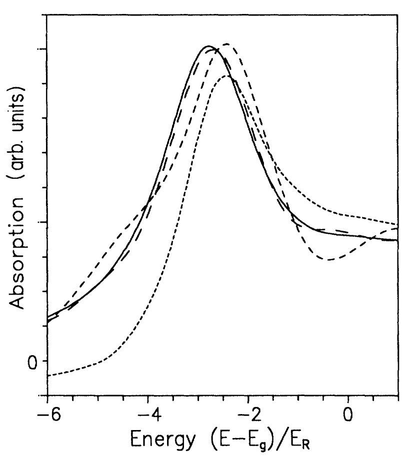

FIG. 7. The numerically evaluated transient behavior of the heavy-hole exciton for a room-temperature 50-Å GaAs MQW. The following parameters were chosen for the simulations: $1.2E_R$ homogeneous broadening of exciton, $7.3E_R$ detuning below the resonance, and 70-fs full width at half maximum (FWHM) pump-pulse intensity duration. The peak-to-valley ratio looks high because the light-hole exciton is ignored in the calculation. The upper solid curve is the linear absorption spectrum, while the long-dashed, short-dashed, and the lower solid curves are for time delays $t_p = 250$, -250, and 0 fs, respectively.

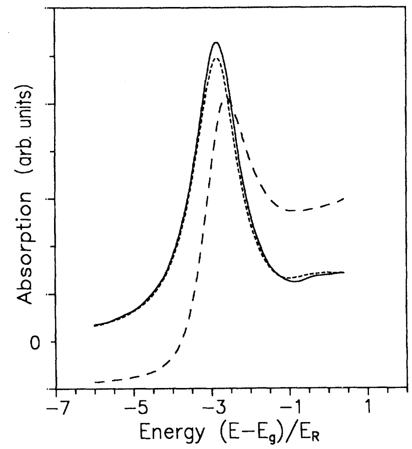

FIG. 8. Calculated absorption spectra for transient behavior of a low-temperature 50-Å GaAs MQW. The following parameters were chosen for the simulations: $0.7E_R$ homogeneous broadening of exciton, $6E_R$ detuning below the resonance, and 150-fs (FWHM) pump-pulse duration. The light-hole exciton was ignored in these calculations. The solid curve represents the linear absorption; the long-dashed curve is for zero time delay between the pump and probe pulses, and the short-dashed curve is plotted for a time delay of $t_p = 500$ fs.

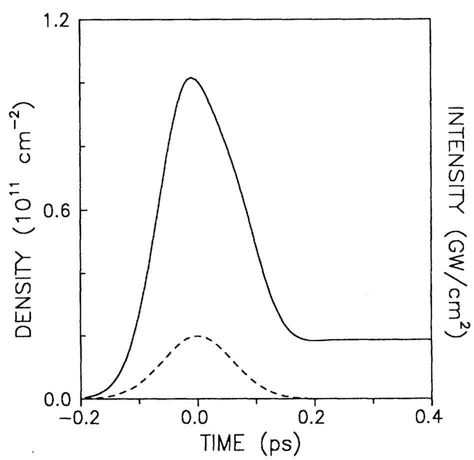

FIG. 9. Calculated temporal behavior of the carrier density generated by pump pulse under the conditions specified in Fig. 7.

semiconductor Bloch equations would still be a very involved task, we have treated this frequency dependence as a parameter. Hence, only the qualitative behavior of the time evolution of the spectrum, and not the quantitative amount of recovery, is correctly taken into account in the numerical solution. Furthermore, a quantitative treatment of the exact recovery would require the inclusion of screening into the Bloch equations, which itself presents a major complication to Eqs. (1) and (2). Here we have restricted ourselves to the case in which the recovery is almost complete, so that excitation of real carriers does not invalidate the neglect of screening. Figure 9 shows the temporal behavior of the created carrier density, which is proportional to $f_{\rm tot}(t)=2\sum_{\bf k} f_{\bf k}(t)$, along with the pump-pulse intensity. Note that similar to the experiments, there is a fast component of the density, which follows the pump, and a small long-lasting tail due to the incoherent component of the real carrier generation. The fast component is a result of the coherent response of the carrier density. It is the transient presence of this density which is responsible for the fast bleaching recovery. We assign this behavior to the ultrafast adiabatic following in semiconductors.

Since our numerical solutions yield the full complex polarization $P(\omega)$, we can easily obtain the nonlinear refractive index $n(\omega)$ from the real part of P. In Fig. 10 we plot an example of the results for the conditions chosen for Fig. 8. The solid line shows the absorption changes $\Delta\alpha$ for a pump-probe delay $t_p=0$, and the dashed curve shows the refractive index changes Δn. It is noted that the Kramers-Kronig relations between $\Delta\alpha$ and Δn are no longer valid in this case because of the fast pulse-excitation conditions. Figure 10 shows that substantial index changes are obtained under the assumed excitation conditions, consistent with the behavior of the NLDC devices that we have presented in Figs. 3–6.

CONCLUSION

In conclusion, we have observed a fast bleaching recovery of the heavy-hole exciton absorption spectrum at room and low temperatures in several GaAs multiple-quantum-well structures and in a MQW nonlinear directional coupler. This coherent feature is a part of the optical Stark effect and manifested in GaAs nonlinear directional coupler as a total transmission increase. Like the blue shift in the optical Stark effect, this behavior can be described by the semiconductor optical Bloch equations. The transient exciton population, which temporally follows the pump pulse, and which is responsible for the fast exciton bleaching and recovery, can be described as adiabatic following in a semiconductor.

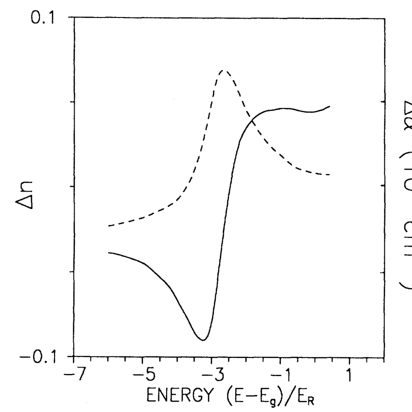

FIG. 10. Calculated absorption changes $\Delta\alpha$ (solid curve) for $t_p=0$ obtained from Fig. 8 and index changes Δn (dashed curve) for the same conditions.

Note added in proof. The recent report on the observation of photocurrents in a $GaAs/Al_xGa_{1-x}As$ quantum well as a result of virtual charge excitation by off-resonant pumping[22] may be also explained by the ultrafast adiabatic following effect we have discussed in this paper.

ACKNOWLEDGMENTS

The authors would like to acknowledge support from the National Science Foundation (Grants Nos. ECS-8822305, ECS-8909913, and EET-8808393), the Army Research Office (Grant No. DAAL03-89-k-0100), the Optical Circuitry Cooperative of the University of Arizona, and a grant for CPU time at the Pittsburgh Supercomputer Center. R.B. acknowledges partial financial support from the DFG (Deutsche Forschungsgemeinschaft, Federal Republic of Germany).

*Also with the Physics Department of the University of Arizona, Tucson, AZ 85721.

[1]P. C. Becker, H. L. Fragnito, C. H. Brito Cruz, R. L. Fork, J. E. Cunningham, J. E. Henry, and C. V. Shank, Phys. Rev. Lett. **61**, 1647 (1989).

[2]D. Fröhlich, A. Nöhte, and K. Reimann, Phys. Rev. Lett. **55**, 1335 (1986).

[3]A. Mysyrowicz, D. Hulin, A. Antonetti, A. Migus, W. T. Masselink, and H. Morkoc, Phys. Rev. Lett. **56**, 2748 (1986).

[4]B. Fluegel, N. Peyghambarian, G. Olbright, M. Lindberg, S. W. Koch, M. Joffre, D. Hulin, A. Migus, and A. Antonetti, Phys. Rev. Lett. **59**, 2588 (1987); see also J. P. Sokoloff, M. Joffre, B. Fluegel, D. Hulin, M. Lindberg, S. W. Koch, A. Migus, A. Antonetti, and N. Peyghambarian, Phys. Rev. B **38**, 7615 (1989).

[5]N. Peyghambarian, S. W. Koch, M. Lindberg, B. Fluegel, and M. Joffre, Phys. Rev. Lett. **62**, 1185 (1990).

[6]W. H. Knox, D. S. Chemla, D. A. B. Miller, J. B. Stark, and S. Schmitt-Rink, Phys. Rev. Lett. **62**, 1189 (1989).

[7]M. Joffre, D. Hulin, J. P. Foing, J. P. Chambaret, A. Migus, and A. Antonetti, IEEE J. Quantum Electron. **25**, 2505 (1989).

[8]L. Allen and J. H. Eberly, *Optical Resonance and Two-Level Atoms* (Wiley, New York, 1975).

[9]D. Grischowsky, Phys. Rev. Lett. **25**, 866 (1971).

[10]R. Binder, S. W. Koch, M. Lindberg, and N. Peyghambarian (unpublished).

[11]M. Lindberg and S. W. Koch, Phys. Rev. B **38**, 3342 (1988); see also S. W. Koch, N. Peyghambarian, and M. Lindberg, J. Phys. C **21**, 5229 (1988) and H. Haug and S. W. Koch, *Quan-*

tum Theory of the Optical and Electronic Properties of Semiconductors (World Scientific, Singapore, 1990).

[12]S. Schmitt-Rink and D. S. Chemla, Phys. Rev. Lett. **57**, 2752 (1986); see also S. Schmitt-Rink, D. S. Chemla, and H. Haug, Phys. Rev. B **37**, 941 (1988).

[13]W. Schäfer, K. H. Schuldt, and R. Binder, Phys. Status Solidi B **150**, 407 (1988).

[14]I. Balslev, R. Zimmermann, and A. Stahl, Phys. Rev. B **40**, 4095 (1989).

[15]R. Zimmermann and M. Hartmann, Phys. Status Solidi B **150**, 365 (1988).

[16]C. Ell, J. F. Müller, K. El-Sayed, and H. Haug, Phys. Rev. Lett. **62**, 304 (1989).

[17]W. H. Knox, R. L. Fork, M. C. Downer, D. A. B. Miller, D. S. Chemla, C. V. Shank, A. C. Gossard, and W. Wiegmann, Phys. Rev. Lett. **54**, 1306 (1986).

[18]S. Schmitt-Rink, D. S. Chemla, and D. A. B. Miller, Adv. Phys. **38**, 89 (1990).

[19]R. Jin, J. P. Sokoloff, P. A. Harten, C. L. Chuang, S. G. Lee, M. Warren, H. M. Gibbs, N. Peyghambarian, J. N. Polky, and G. A. Pubanz, Appl. Phys. Lett. **56**, 993 (1981); see also R. Jin, C. L. Chuang, H. M. Gibbs, S. W. Koch, J. N. Polky, and G. A. Pubanz, *ibid.* **53**, 1791 (1988).

[20]R. Hoffe and J. Chrostowski, Opt. Commun. **57**, 34 (1986).

[21]S. Trillo, S. Wabnitz, N. Finlayson, W. C. Banyai, C. T. Seaton, G. I. Stegeman, and R. H. Stolen, Appl. Phys. Lett. **53**, 837 (1988).

[22]Y. Sakata, M. Yamanishi, Y. Yamaoka, S. Kodama, Y. Kan, and I. Suemune, Jpn. J. Appl. Phys. (to be published).